Cell Stem Cell
Article

p57^{Kip2} and p27^{Kip1} Cooperate to Maintain Hematopoietic Stem Cell Quiescence through Interactions with Hsc70

Peng Zou,[1,*] Hiroki Yoshihara,[1] Kentaro Hosokawa,[1] Ikue Tai,[1] Kaori Shinmyozu,[2] Fujiko Tsukahara,[3] Yoshiro Maru,[3] Keiko Nakayama,[4] Keiichi I. Nakayama,[5] and Toshio Suda[1,*]
[1]Department of Cell Differentiation, The Sakaguchi Laboratory of Developmental Biology, Keio University School of Medicine, Shinjuku-ku, Tokyo 160-8582, Japan
[2]Proteomics Support Unit, RIKEN Center for Developmental Biology, Kobe Hyogo 650-0047, Japan
[3]Department of Pharmacology, Tokyo Women's Medical University School of Medicine, Shinjuku-ku, Tokyo 162-8666, Japan
[4]Department of Developmental Genetics, Center for Translational and Advanced Animal Research, Graduate School of Medicine, Tohoku University, Sendai 980-8575, Japan
[5]Department of Molecular and Cellular Biology, Medical Institute of Bioregulation, Kyushu University, Fukuoka 812-8582, Japan
*Correspondence: zoupeng@sc.itc.heio.ac.jp (P.Z.), sudato@sc.itc.keio.ac.jp (T.S.)
DOI 10.1016/j.stem.2011.07.003

SUMMARY

Cell cycle regulators play critical roles in the balance between hematopoietic stem cell (HSC) dormancy and proliferation. In this study, we report that cell cycle entry proceeded normally in HSCs null for cyclin-dependent kinase (CDK) inhibitor p57 due to compensatory upregulation of p27. HSCs null for both p57 and p27, however, were more proliferative and had reduced capacity to engraft in transplantation. We found that heat shock cognate protein 70 (Hsc70) interacts with both p57 and p27 and that the subcellular localization of Hsc70 was critical to maintain HSC cell cycle kinetics. Combined deficiency of p57 and p27 in HSCs resulted in nuclear import of an Hsc70/cyclin D1 complex, concomitant with Rb phosphorylation, and elicited severe defects in maintaining HSC quiescence. Taken together, these data suggest that regulation of cytoplasmic localization of Hsc70/cyclin D1 complex by p57 and p27 is a key intracellular mechanism in controlling HSC dormancy.

INTRODUCTION

HSCs play an essential role in the maintenance of multiple lineages of blood cells through their dual ability to self-renew and to differentiate into progenitors of various lineages. By protecting HSCs from proliferative exhaustion, cell cycle quiescence is essential for the long-term engraftment potential and maintenance of stem cells. A balance of cell-extrinsic and -intrinsic regulators normally maintains HSCs in a state of relative dormancy. Our previous studies indicate that HSC quiescence is regulated by several extracellular factors, including Ang1/Tie2 (Arai et al., 2004), THPO/MPL (Yoshihara et al., 2007), and N-cadherin/β-catenin (Hosokawa et al., 2010). Because these pathways must converge on cell cycle regulation, it might be possible to drive HSC fate determination by directly manipulating the expression of intracellular cell cycle regulators. However, little is known about the intracellular mechanisms of cell cycle factors that regulate HSC quiescence and proliferation.

An early stage of the cell cycle is regulated by the action of the D-type cyclins that, together with their catalytic partner CDKs, function as intracellular sensors of extracellular signals. Their activities are carefully regulated by the INK4 family (p15, p16, p18, p19) and the Cip/Kip family (p21, p27, p57) of CDK inhibitors. Both positive and negative cell cycle regulators, including the D-type cyclins (Kozar et al., 2004), Cdk4/6 (Malumbres et al., 2004), and the INK4 family of CDK inhibitors (Oguro et al., 2006; Yuan et al., 2004), are critical for various aspects of HSC proliferation. In the Cip/Kip family gene products, p21 is critical for preventing HSC exhaustion by regulating quiescence (Cheng et al., 2000b), whereas p27 regulates the proliferation and pool size of hematopoietic progenitor cells (HPCs) rather than that of HSCs (Cheng et al., 2000a).

Among all CDK inhibitors, p57 is unique because of its essential role in development (Pateras et al., 2009). Recent studies have shown that p57 is highly expressed in the Thy1.1^{int}Flk2^{-}LSK (Passegué et al., 2005) and CD34^{-}MPL^{+}LSK (Yoshihara et al., 2007) quiescent populations of HSCs. Furthermore, TGF-β-induced cell cycle arrest in HPCs (Scandura et al., 2004) and HSCs (Yamazaki et al., 2009) is correlated with an increase in p57 expression. These observations suggest that HSC quiescence is potentially maintained by the modulation of p57 expression. However, the role of p57 in HSCs has not been determined, because of the neonatal lethality of *p57*$^{-/-}$ mice.

In this study, p57 was found to contribute to the maintenance of HSC quiescence, and p27 compensated for p57 function in HSCs with a p57 deletion. An association between p57, p27, and Hsc70 was found to maintain the cytoplasmic localization of the Hsc70/cyclin D1 complex and regulate the cell cycle entry of HSCs. These findings provide insights into the physiological function of p57 and p27 in HSCs and have implications for the roles of CDK inhibitors in the maintenance of tissue homeostasis.

RESULTS

Deletion of p57 in Embryonic HSCs Did Not Affect Cell Cycle Progression

Bone marrow (BM) lineage$^-$ Sca1$^+$ c-Kit$^+$ (LSK) cells can be divided into populations of long-term reconstituting HSCs (LT-HSCs; CD34$^-$/Flt3$^-$ or CD150$^+$/CD48$^-$), which are capable of extensive self-renewal, and short-term reconstituting HSCs (ST-HSCs; CD34$^+$/Flt3$^-$ or CD150$^-$/CD48$^-$), which self-renew for a limited time before giving rise to a population of non-self-renewing multipotent progenitors (MPPs; CD34$^+$/Flt3$^+$ or CD48$^+$) (Adolfsson et al., 2001; Kiel et al., 2005). To gain insights into G_0/G_1 cell cycle control in these populations, we analyzed the expression levels of G1 phase cyclins via qRT-PCR. Within the pool of LSK cells, LT-HSCs expressed the highest levels of cyclin D1 and D2 and the lowest levels of cyclin D3 (Figure 1A). However, no induction of cyclin E1 or E2 was observed in LT-HSCs, although their expression is correlated with cyclin D-dependent Rb-mediated transcription. Furthermore, both of the G_1 phase CDKs were expressed at low levels in LT-HSCs (Figure 1B). In contrast, the differentiation of LT-HSC into ST-HSC and then into MPP specifically correlated with decreased expression of p57 and increased expression of p21, whereas p27 expression did not change significantly (Figure 1C).

Immunocytochemistry showed that most Ki67$^-$LSK cells (quiescent HSCs) exhibited abundant expression of p57 in the cytoplasm, whereas most Ki67$^+$LSK cells (cycling HSCs or MPPs) showed only weak expression of p57. In contrast, no significant difference in the expression of p21 or p27 was detected between Ki67$^-$ and Ki67$^+$LSK cells (see Figure S1A available online). To understand how cell cycle entry is regulated in HSCs, freshly isolated CD34$^-$LSK cells were stimulated with SCF (stem cell factor). SCF stimulation caused the degradation of p57 and nuclear translocation of cyclin D1, which were followed by Rb phosphorylation (Figure S1B). Interestingly, CDK2, CDK4, and CDK6 were not detected in the cytoplasm of CD34$^-$LSK cells although their nuclear expression was induced after SCF stimulation (Figure S1C and data not shown). These results suggest that p57 in HSCs may regulate cell cycle progression by controlling the subcellular localization of cyclin D, which is independent of the expression of the CDKs.

To investigate whether the proliferation of hematopoietic cells was affected by p57 deficiency, cell cycle progression was examined in fetal liver (FL) LSK cells, common lymphoid progenitors (CLP), common myeloid progenitors (CMP), granulocyte-macrophage progenitors (GMP), and megakaryocyte-erythroid progenitors (MEP) (Figure S2A). Hoechst staining showed that the absence of p57 did not affect the proliferation of FL LSK cells or progenitors (Figure S2B). In addition, no significant difference was detected in the total number of LSK cells between $p57^{+/+}$ and $p57^{-/-}$ embryos (Figure S2C).

Next, in vitro colony-forming assays were performed with freshly isolated FL Flt3$^-$ or Flt3$^+$LSK cells. Equal numbers of $p57^{+/+}$ or $p57^{-/-}$ cells were plated, and equivalent numbers of colonies were generated (Figure 2A). To determine whether p57 is involved in adult BM HSC reconstitution, the long-term repopulating capacity of $p57^{-/-}$ FL HSCs was examined in vivo. Flow cytometric analysis of the peripheral blood (PB) of the transplant recipients revealed that $p57^{+/+}$ and $p57^{-/-}$ FL LSKs were equally capable of supplying hematopoietic cells (Figure 2B). Serial BMTs also were performed to analyze the self-renewal capacity of $p57^{-/-}$ HSCs. Examination of donor-derived BM (Figure 2C) or LSK (Figure 2E) cells after the third transplantation revealed a substantial reduction in the reconstitution capacity of $p57^{-/-}$ HSCs compared to $p57^{+/+}$ HSCs. The proliferation of donor-derived LSK cells was then determined by Ki67 staining (Figure 2D). There was no difference in the frequency of G_0 cells between $p57^{+/+}$ and $p57^{-/-}$ LSK cells at either the first or the third BMT (Figure 2F). These data indicate that p57 may mediate the self-renewal capacity of FL donor-derived HSCs during serial BMT, but that the changes are not caused by alterations in the cell cycle.

Deficiency of p57 Leads to the Upregulation of p27 in HSCs

Although p57 deficiency did not affect the maintenance of quiescence in HSCs, molecular redundancy or compensatory mechanisms may exist that compensate for the loss of p57. The expression of CDK inhibitors was examined in LSK cells isolated from $p57^{+/+}$ or $p57^{-/-}$ donor-derived BM at 4 months post-BMT. The effects of THPO administration on gene expression in donor-derived LSK cells of recipient mice was also investigated (Figure 3A) because THPO/MPL signaling is involved in the maintenance of HSC quiescence and is associated with the regulation of p57 signaling pathways in HSCs (Yoshihara et al., 2007). Consistent with previous studies, upregulation of p57 occurred in wild-type (WT) donor-derived LSK cells after 3 days of daily THPO administration. Interestingly, a significant increase in p27 expression was detected in $p57^{-/-}$ LSK cells, and the increase became more distinct after THPO administration, whereas p21 expression was the same in all groups (Figure 3B). In addition, $p57^{-/-}$ LSK cells exhibited a greater level of p18 expression, which is correlated with the self-renewal of HSCs (Yuan et al., 2004). However, THPO administration did not increase the expression of p18 in $p57^{-/-}$ LSK cells, indicating a difference between the regulation of p18 and p27.

In the serial BMT, p18, but not p27, was upregulated in the reconstituted $p57^{-/-}$ LSK cells during the transplantation (Figure 3C). Furthermore, $p57^{-/-}$ donor-derived CD34$^-$LSK cells showed a high level of p18 expression in the nucleus (Figure 3D; Figure S3A), whereas, in contrast, p27 was expressed predominantly in the cytoplasm of these cells (Figure 3E; Figure S3B). In addition, the upregulation of p21 expression in donor-derived LSK cells was not observed when p57 was deleted (Figure S3C). Taken together, these data suggest that p27 may compensate for the loss of p57 function in the cytoplasm for the maintenance of quiescence in $p57^{-/-}$ HSCs.

Critical Role of p57 in the Maintenance of $p27^{-/-}$ BM LSK Cells

Given the upregulation of p27 in $p57^{-/-}$ FL donor-derived HSCs at post-BMT, a p57 knockdown (KD) strategy was utilized in $p27^{-/-}$ adult BM LSK cells to reduce the expression of p57 in the absence of p27 (Figure 4A). As shown in Figure S4A, the expression of p57 in $p27^{-/-}$ LSK cells was not affected. Three retroviral p57 shRNAs were introduced into MEFs, and the efficient reduction of p57 expression by sh-1 was verified (Figure S4B). LSK cells were isolated from $p27^{+/+}$

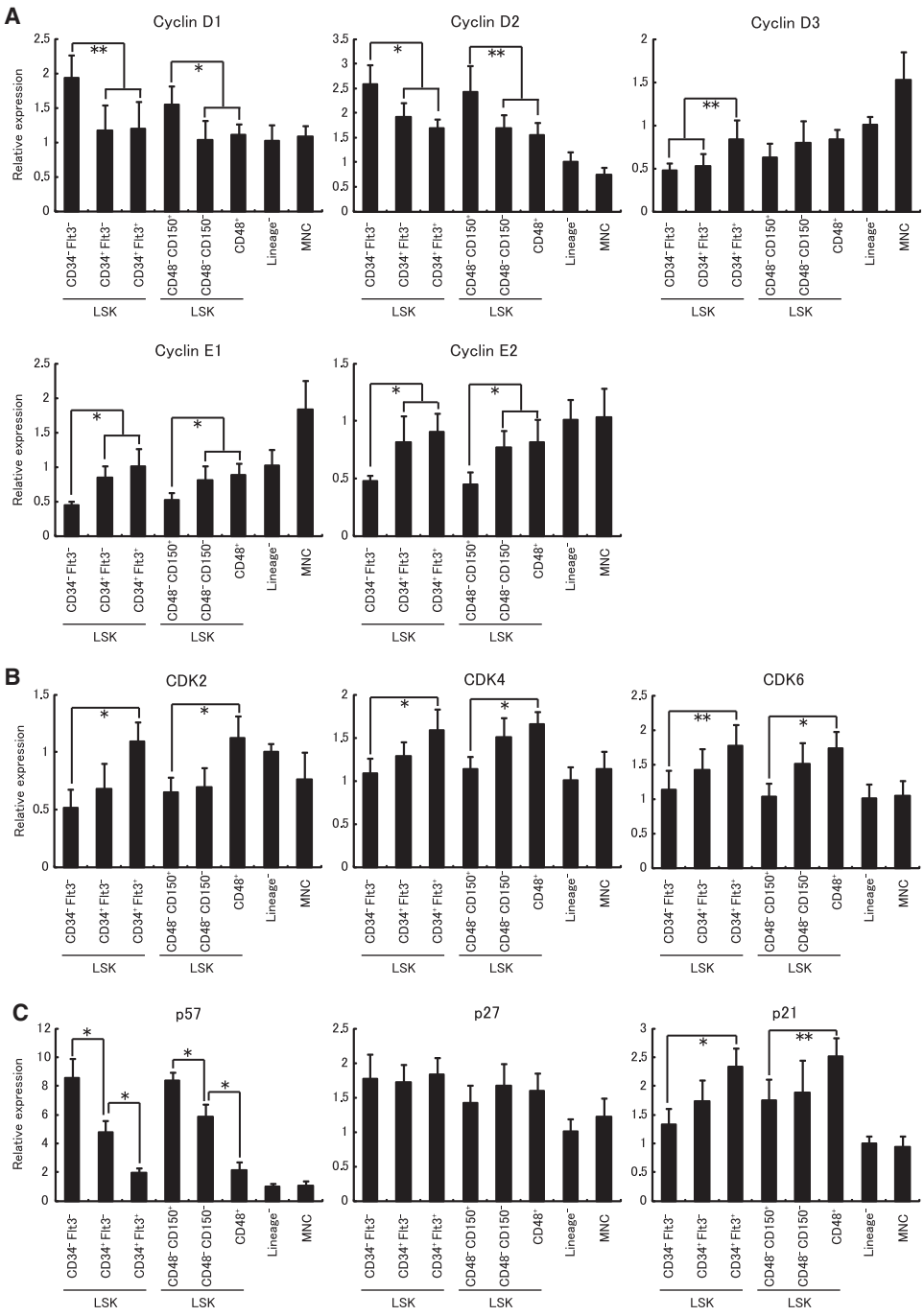

Figure 1. qRT-PCR Analysis of Cell Cycle-Related Genes in LT-HSC, ST-HSC, MMP, Lineage$^-$, and MNC Fractions

LT-HSC, ST-HSC, and MMP fractions are from CD34$^-$/Flt3$^-$ or CD48$^-$/CD150$^+$; CD34$^+$/Flt3$^-$ or CD48$^-$/CD150$^-$; and CD34$^+$/Flt3$^+$ or CD48$^+$ populations, respectively.

(A) Expression levels of G_1 phase cyclins.

(B) Expression levels of G_1 phase CDKs.

(C) Expression levels of the p21, p27, and p57 CDK inhibitors.

Data represent mean values from three samples, all performed in duplicate. Error bars indicate the SD (*$p < 0.01$, **$p < 0.05$, $n = 3$).

or *p27*$^{-/-}$ BM and were transduced with either the scrambled control (CON) or the p57 sh-1 KD vector. At day 2 after viral infection, each group of LSK GFP$^+$ cells was sorted for functional assessment.

Long-term colony-initiating cell (LTC-IC) assays were first performed for GFP$^+$ cells on a layer of OP9 stromal cells. In this assay, the number of colony-forming cells after 6 weeks of culture reflects HSC function. After 6 weeks, the number of

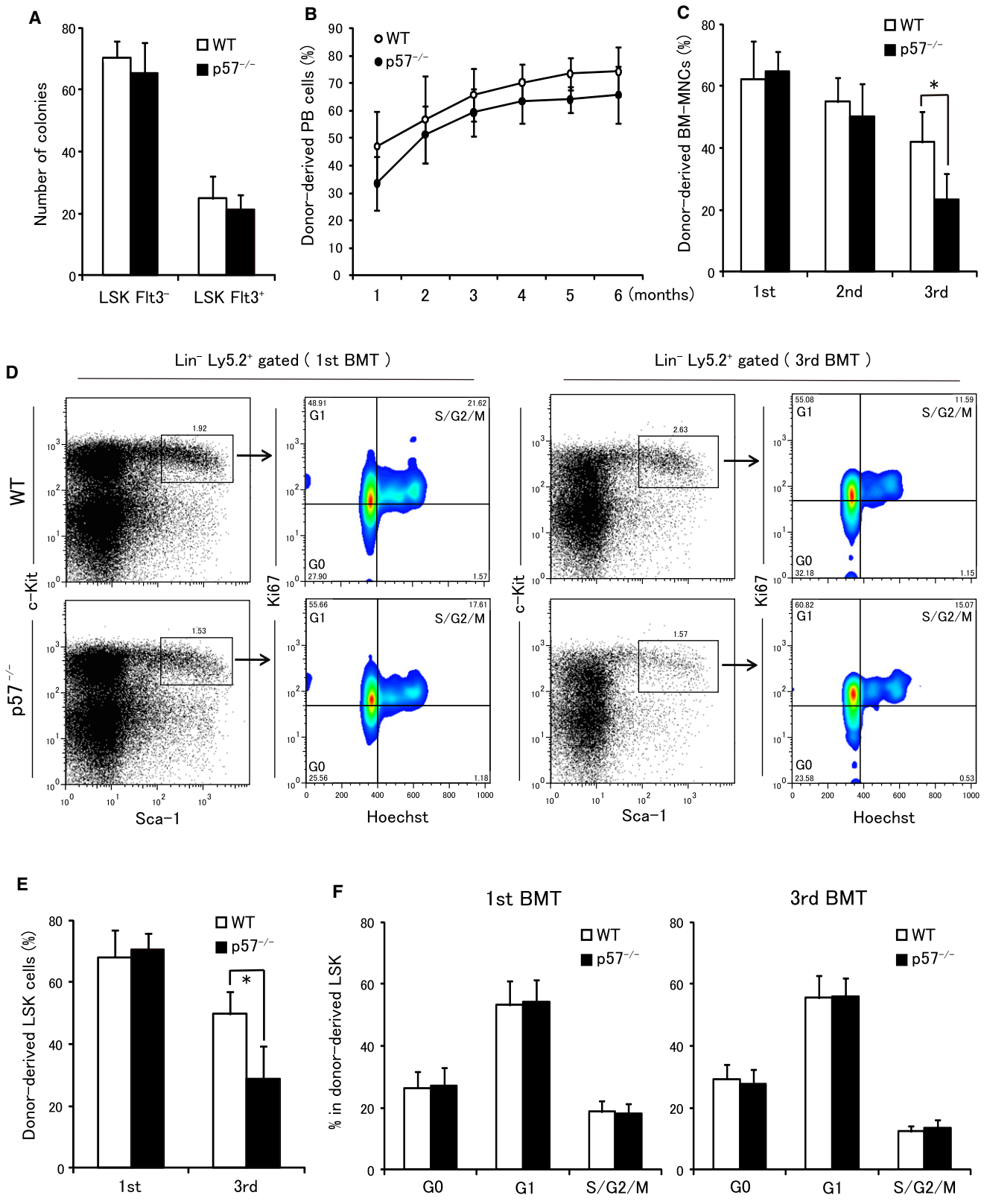

Figure 2. p57 Deficiency Affects HSC Repopulating Ability upon Serial BMT, but Is Not Caused by an Altered Cell Cycle

(A) Normal clonogenic capacity of *p57*$^{-/-}$ FL HSCs in vitro. Flt3^{-} or Flt3^{+} LSK cells were flow sorted from *p57*$^{+/+}$ or *p57*$^{-/-}$ E14.5 FLs and cultured in methylcellulose medium for 7 days. Data shown are the mean number of colonies (±SD) formed per 200 cells (n = 3).

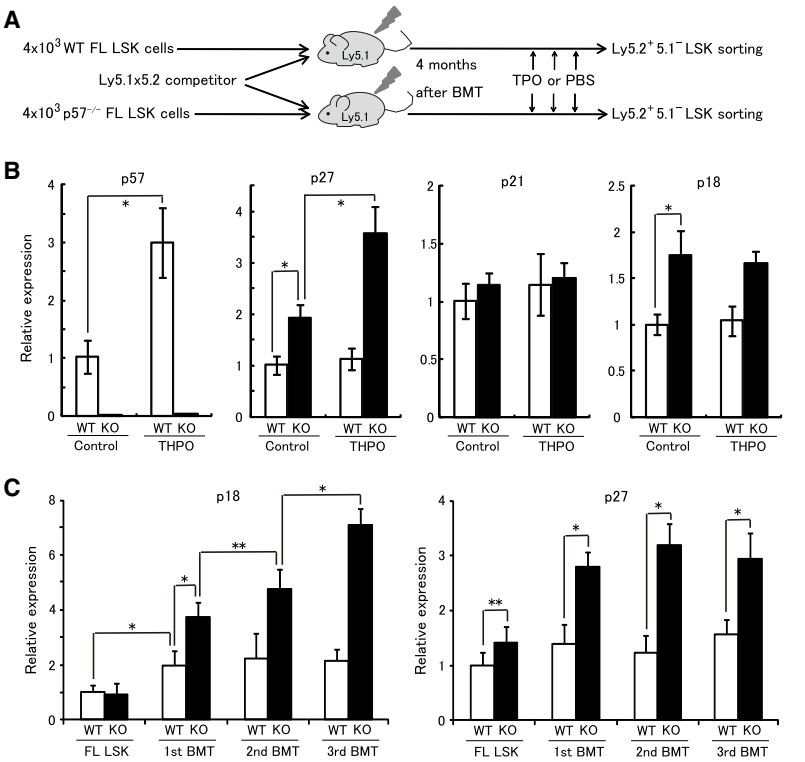

Figure 3. Expression of CDK Inhibitors in $p57^{+/+}$ or $p57^{-/-}$ FL Donor-Derived LSK Cells after Transplantation

(A) Scheme of the preparation of donor-derived LSK cells.

(B) Increased p27 and p18 expression in $p57^{-/-}$ LSK cells at 4 months posttransplantation. Donor-derived LSK cells were sorted after 3 days of daily THPO or PBS (control). The relative expression of CDK inhibitors (p21, p27, p57, and p18) was analyzed by qRT-PCR. Data shown are mean (±SD) values from two independent experiments (*$p < 0.01$, $n = 3$).

(C) Increased p18 expression in $p57^{-/-}$ LSK cells during serial BMT. FL LSK cells before transplantation or FL donor-derived LSK cells were sorted after each BMT. The relative expression of p18 and p27 was analyzed. Data shown are mean (±SD) values from two independent experiments (*$p < 0.01$, **$p < 0.05$, $n = 3$).

(D) Expression of p18 was upregulated in the nucleus of $p57^{-/-}$ donor-derived $CD34^-$LSK cells at 4 months posttransplantation. Freshly isolated donor-derived cells were stained with anti-p18 (green) and DAPI (blue).

(E) Expression of p27 was upregulated in the cytoplasm of $p57^{-/-}$ donor-derived $CD34^-$LSK cells at 4 months posttransplantation. Freshly isolated donor-derived cells were stained with anti-p27 (green) and DAPI (blue).

colonies derived from $p27^{-/-}p57^{KD}$ LSK cells was significantly less than that derived from $p27^{+/+}p57^{CON}$, $p27^{+/+}p57^{KD}$, or $p27^{-/-}p57^{CON}$ LSK cells, although there was no significant difference in the short-term cultures (less than 2 weeks) (Figure 4B). In addition, almost no large LTC-IC colonies (>2 mm in diameter) were generated from $p27^{-/-}p57^{KD}$ LSK cells (Figure S4C). Because these colonies represent the more primitive hematopoietic cell populations, these data suggest that p57 and p27 cooperate to maintain the immature HSC phenotype in vitro.

To evaluate HSC function in vivo, the repopulating capacity of $p27^{-/-}p57^{KD}$ LSK cells was next examined via competitive reconstitution assays. The $p27^{-/-}p57^{KD}$ cell recipients showed low donor-derived cell chimerism in the PB at 2 months after transplantation, and this proportion decreased thereafter. In contrast, the transplanted $p27^{+/+}p57^{CON}$, $p27^{+/+}p57^{KD}$, or $p27^{-/-}p57^{CON}$ cells showed a steady increase in chimerism from 2 to 4 months posttransplantation (Figure 4C). These results indicate that $p57^{KD}$ may cause an in vivo defect that impairs the function of LSK cells after BMT when p27 expression is deficient. To characterize the defect in $p27^{-/-}p57^{KD}$ LSK cells, the homing capacity and viability of transplanted cells were tested. 30 hr after BMT, homing capacity and apoptotic cell ratio of transplanted GFP^+ cells in the BM were equivalent in each group (Figures S4D and S4E). Therefore,

(B) Normal long-term reconstitution capacity of $p57^{-/-}$ FL LSK cells. Irradiated recipient mice were transplanted with 4×10^3 LSK cells from $p57^{+/+}$ or $p57^{-/-}$ FLs plus 2×10^5 BM-MNCs. Data shown are the mean percentages (±SD) of donor-derived cells in the PB at the indicated times after transplantation ($n = 5$).

(C) Defective repopulation capacity of $p57^{-/-}$ BM MNCs during serial transplantation. 4×10^3 donor-derived LSK cells from the recipient mice were serially transplanted into recipient mice. The repopulating capacity of $p57^{+/+}$ or $p57^{-/-}$ donor cells was determined at 16 weeks posttransplant for each BMT. Data shown are the mean percentages (±SD) of donor-derived cells in BM MNCs (*$p < 0.01$, $n = 5$).

(D) Equivalent cell cycle status of posttransplant $p57^{+/+}$ and $p57^{-/-}$ LSK cells. Results shown are one analysis representative of two independent experiments.

(E) Defective repopulation of $p57^{-/-}$ LSK cells derived from BM cells in serial transplantation. BM cells from the recipient mice were analyzed for the frequency of donor-derived LSK cells at 16 weeks post-BMT (±SD, *$p < 0.01$, $n = 5$).

(F) Cell cycle status in the pool of donor-derived LSK cells. Cell cycle analyses of LSK populations by Ki67 and Hoechst staining in (D). The percentages of cells in G_0, G_1, or $S/G_2/M$ phase are indicated (±SD).

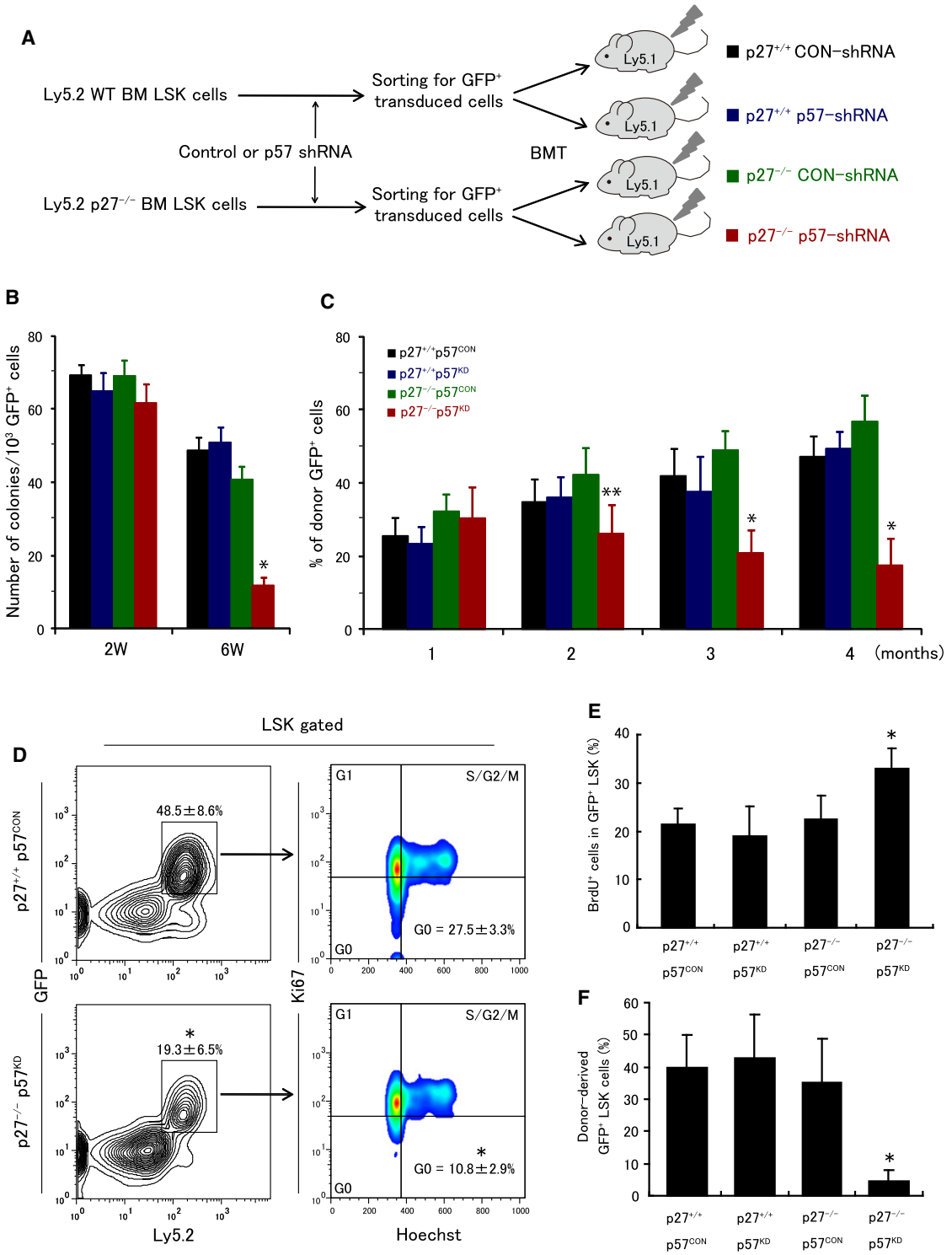

Figure 4. Abrogated Self-Renewal Capacity and Defective Maintenance of Quiescence in *p27*$^{-/-}$*p57*^{KD} LSK Cells

(A) The experimental scheme for shRNA transduction.

(B) Decreased colony formation of *p27*$^{-/-}$*p57*^{KD} LSK cells after long-term culture. *p27*$^{+/+}$*p57*^{CON}, *p27*$^{+/+}$*p57*^{KD}, *p27*$^{-/-}$*p57*^{CON}, or *p27*$^{-/-}$*p57*^{KD} GFP$^+$ LSK cells (2×10^3) were cultured on OP9 stromal cells for the indicated number of weeks (W) and tested for colony formation. Data shown are the mean number (±SD) of colonies formed (*$p < 0.01$, $n = 3$).

(C) Hematopoietic reconstitution capacity of *p27*$^{+/+}$*p57*^{CON}, *p27*$^{+/+}$*p57*^{KD}, *p27*$^{-/-}$*p57*^{CON}, and *p27*$^{-/-}$*p57*^{KD} LSK cells. Irradiated recipient mice were transplanted with 5×10^3 GFP$^+$ LSK cells and 2×10^5 competitor cells. Data shown are the mean percentages (±SD) of donor GFP$^+$ cells in the PB at the indicated time-points post-BMT (*$p < 0.01$, **$p < 0.05$, $n = 5$).

the engraftment defect of $p27^{-/-}p57^{KD}$ LSK cells cannot be attributed to a defect in homing or cell survival.

It was next investigated whether the repopulating defect observed with $p27^{-/-}p57^{KD}$ LSK cells could result from changes in their cell cycle distribution. Analysis of donor-derived GFP^+ cells revealed that $p27^{-/-}p57^{KD}$ LSK cells had a 2-fold decrease in the frequency of $Ki67^-$ quiescent cells (Figure 4D) and a correlative increase in the percentage of $BrdU^+$ cycling cells (Figure 4E). Thus, a proportion of quiescent LSK cells in the BM are profoundly affected by the loss of p57 when p27 is unavailable. Furthermore, examination of donor-derived GFP^+ LSK cells after the second transplantation revealed a severe reduction in the self-renewal capacity of $p27^{-/-}p57^{KD}$ HSCs (Figure 4F).

Failure to Maintain Quiescence in $p27^{-/-}p57^{-/-}$ HSCs

Hematopoietic cells are rapidly expanded in the FL; however, FL $EPCR^+$LSK cells are represented in a slow cycling population as early as E12.5 (Iwasaki et al., 2010). To confirm the genetic cooperation of p57 and p27 in regulating HSC proliferation, the cell cycle of E14.5 FL $CD48^-EPCR^+$LSK cells was examined in $p27^{-/-}p57^{-/-}$ (DKO) mice. Loss of both p27 and p57 significantly decreased the frequency of $Ki67^-$ HSCs compared to the frequency in $p27^{-/-}$, $p57^{-/-}$, or WT mice (Figure S5A). However, no significant differences were detected in the total cell numbers of LSK and progenitors between DKO embryos and the other genotypes (Figure S5B). Furthermore, DKO FL $CD48^-EPCR^+$LSK cells showed no defects in colony formation after 7 days in methylcellulose culture (Figure S5C).

Next, the repopulation capacity of FL $CD48^-EPCR^+$LSK cells of various genotypes was examined after BMT. In the short-term (4 and 8 weeks post-BMT), the repopulating capacity of DKO donor-derived cells was comparable to that of other genotypes, and no alteration was observed to suggest that loss of p27 and p57 affects progenitor function (Figure 5A). However, at later time points, the repopulating capacity of DKO cells was lower than that of the control groups. In addition, the number of DKO donor-derived LSK cells sharply decreased at 4 months post-BMT (Figure 5B). These results indicate that deficiency of p27 and p57 may affect the function of HSCs but not that of progenitor cells. In fact, there was a significant reduction in the frequency of $CD48^-CD150^+$LSK cells in reconstituting DKO BM compared to that in controls (Figure 5C). This decrease was not associated with changes in the apoptotic rates of these cells (data not shown).

Based on these observations, the cell cycle profile of reconstituting subpopulations of HSCs ($CD48^-CD150^+$LSK cells) and HPCs ($CD48^+$LSK cells) was further tested. DKO HSCs, while decreased in number, displayed enhanced proliferation, while DKO HPCs did not cycle more than the control groups (Figure 5D). On the other hand, flow cytometric analyses identified an increased number of myeloid ($Mac\text{-}1^+$ and $Gr\text{-}1^+$) cells as well as a reduction in the number of B ($B220^+$) cells in DKO donor-derived BM cells; in contrast, an increased number of T ($CD4^+CD8^+$) cells was detected in both $p27^{-/-}$ and DKO cells (Figure 5E). Despite the perturbed frequency of HSCs and various hematopoietic cell lineages in reconstituting DKO BM, no significant extramedullary hematopoiesis was detected because the spleen size and the frequency of splenic LSK cells in DKO cell recipients were similar to those in other genotypic cell recipients (Figure S5D and data not shown). Specifically, the deficiency of both p57 and p27 in HSCs resulted in a complete lack of long-term maintenance of HSCs after serial BMT (Figure 5F), suggesting that these proteins cooperate to play a pivotal role in the maintenance of HSC quiescence and to protect HSCs from loss of self-renewal activity.

Identification of Hsc70 as a p57 Binding Protein in Quiescent Hematopoietic Cells

Given our in vivo studies suggesting that p57 and p27 cooperate to maintain quiescence in HSCs, p57/p27 binding factors were investigated to elucidate the mechanism of this cooperation. Murine EML cells, a hematopoietic progenitor cell line, were used to identify p57 binding proteins. As previously reported (Ye et al., 2005), $lineage^-$ EML cells can be separated into two populations based on the cell surface marker CD34, and both populations contain similar levels of c-kit. In addition, it was found that the $CD34^+$ population was active in cell cycling, whereas the $CD34^-$ cells were in G_0/G_1 cell cycle arrest, as indicated by Ki67 staining (Figure 6A). It was also observed that p57 was expressed at high levels in $CD34^-$EML cells, while increased c-Myc was detected in $CD34^+$EML cells, correlating with the cell cycle status (Figure S6A).

To identify proteins that physically associate with p57 in quiescent EML cells, p57 binding proteins were coimmunoprecipitated on anti-Myc agarose beads from whole cell extracts of Lin^-CD34^- EML cells overexpressing Myc-p57. Several proteins coprecipitated with Myc-p57 that were absent in the control purification (Figure 6B). Protein bands were excised, digested with trypsin, and subjected to Nano-liquid Chromatography-Tandem Mass Spectrometry (LC-MS/MS). Cyclin D1, D2, CDK4, and CDK6 were identified as prominent copurifying proteins. In addition, the mass spectra identified several tryptic peptides that were identical to murine Hsc70. Also, Hsc70 was detected as an endogenous binding protein of p57 by immunoprecipitation with p57- or Hsc70-specific antibodies in Lin^-CD34^- EML cell lysates (Figure 6C).

Hsc70 is a member of the heat shock protein 70 (Hsp70) family, which shuttles between the cytoplasm and the nucleus and serves as a molecular chaperone for the nuclear import of certain proteins. Diehl et al. (2003) showed that Hsc70 directly

(D) Defective maintenance of quiescence in $p27^{-/-}p57^{KD}$ LSK cells. Cell cycle analysis of GFP^+ donor-derived LSK cells was performed by staining with Hoechst and Ki67 at 16 weeks post-BMT. Inserts show the mean percentages (±SD) of donor-derived GFP^+ LSK cells (*$p < 0.01$, $n = 5$).
(E) Increased $BrdU^+$ cells in $p27^{-/-}p57^{KD}$ LSK cells. Recipient mice were intraperitoneally injected with 1 mg of BrdU at 16 weeks post-BMT. Twenty-four hours after injection, BM MNCs were harvested and stained with surface markers and BrdU antibodies and then analyzed by flow cytometry. The percentages (±SD) of $BrdU^+$ cells in donor-derived LSK cells are indicated (*$p < 0.01$, $n = 5$).
(F) Defective repopulation capacity of $p27^{-/-}p57^{KD}$ LSK cells in second BMT. Donor-derived GFP^+ LSK cells (5×10^3) were obtained from recipient mice and transplanted into sublethally irradiated mice. Data shown are the mean percentages (±SD) of donor-derived GFP^+ LSK cells at 16 weeks after the second BMT (*$p < 0.01$, $n = 5$).

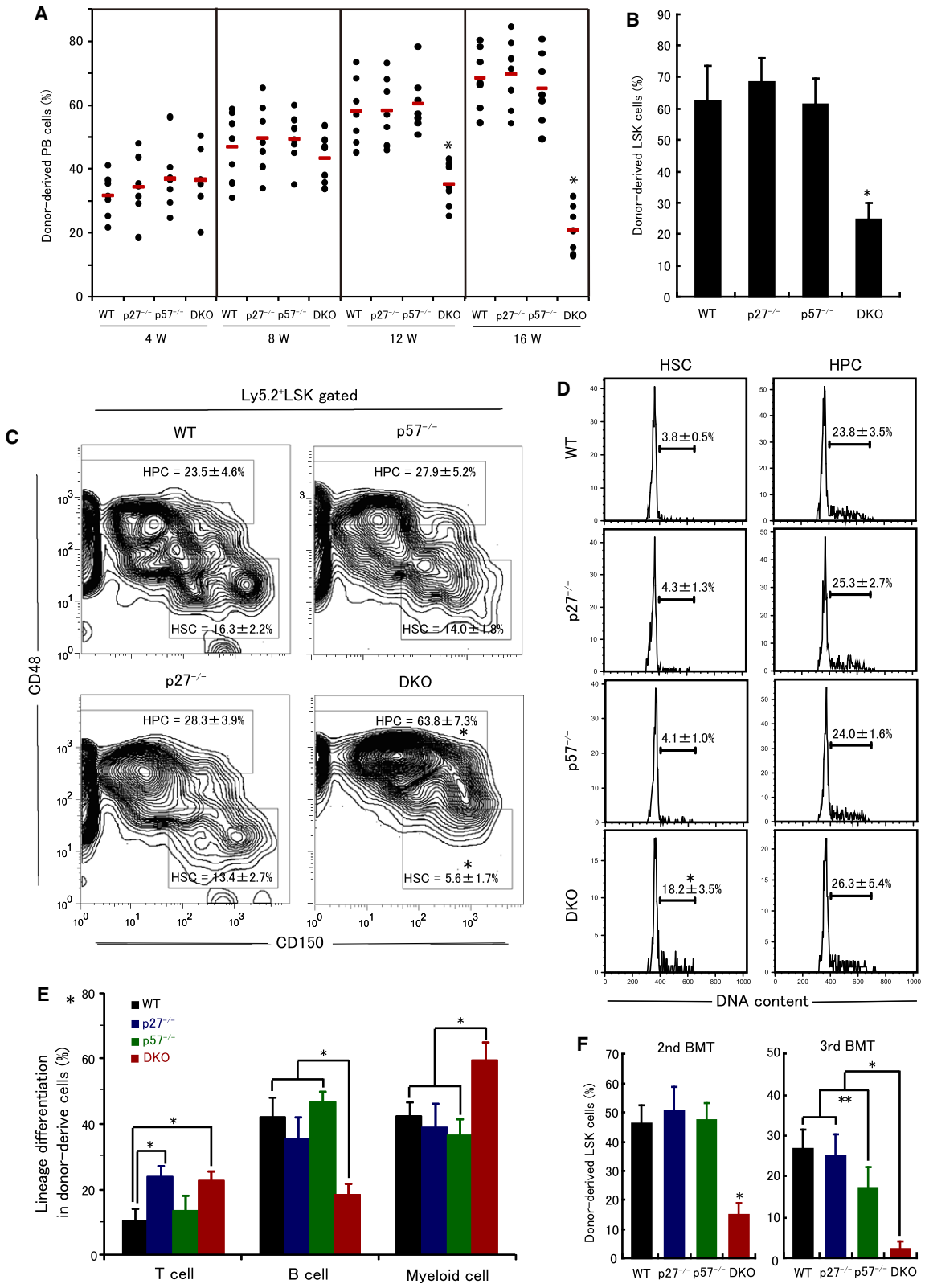

Figure 5. Defects in the Maintenance of Quiescence and the Self-Renewal Capacity of *p27*$^{-/-}$*p57*$^{-/-}$ HSCs

(A) Defective hematopoietic repopulating activity of DKO FL HSCs. 5 × 10^2 FL CD48$^-$EPCR$^+$LSK cells from WT, *p27*$^{-/-}$, *p57*$^{-/-}$, or DKO mice were transplanted into irradiated recipients together with 2 × 10^5 BM-MNC competitors. Red lines indicate the mean percentages of donor-derived PB cells (*p < 0.01, n = 7).

interacts with cyclin D1 and accelerates its binding to CDK4/6 during the G_0/G_1-S transition. Hsc70 is constitutively expressed in the absence of stress in mature mammalian cells and is abundantly expressed in embryonic, mesenchymal, and neural stem cells (Baharvand et al., 2007). The relative levels of Hsc70 mRNA were examined in hematopoietic cells, and Hsc70 was found to be highly expressed in multipotent LSK cells (Figure S6B). In contrast, Hsp70-1a, a member of the Hsp70 family whose expression is induced by stressors such as heat, is expressed at low levels in LSK cells (Figure S6C). The subcellular localization of cyclin D1 and Hsc70 in $CD34^-$LSK cells was next analyzed by immunocytology. Cyclin D1 colocalized with Hsc70 in the cytoplasm of untreated $CD34^-$LSK cells but translocated into the nucleus with Hsc70 after SCF stimulation (Figure S6D). These results suggest that the localization of Hsc70 to the cytoplasm of HSCs may inhibit the G_0/G_1-S transition by regulating the subcellular localization of cyclin D1.

To determine whether other CDK inhibitors bind to Hsc70, expression vectors encoding EGFP-tagged Hsc70 and HA-tagged p21, p27, or p57 were cotransfected into COS-7 cells. EGFP-Hsc70 was immunoprecipitated with anti-GFP from the cell lysates, and immunoblotting was carried out with HA or GFP antibodies. HA-p57 and HA-p27, but not HA-p21, coprecipitated with EGFP-Hsc70 (Figure 6D), suggesting that p57 and p27 may specifically interact with Hsc70 to regulate cell cycle progression in HSCs. Consistent with this, the hyperphosphorylation of Rb in DKO HSCs correlated with the nuclear import of the Hsc70/cyclin D1 complex in donor-derived $CD34^-$LSK cells (Figure 6E). These observations suggest that loss of p57 and p27 in HSCs results in Rb phosphorylation and causes cell cycle entry by regulating the nuclear import of the Hsc70/cyclin D1 complex.

Control of the Cytoplasmic Hsc70/Cyclin D1 Complex Is a Key Molecular Mechanism of HSC Quiescence

Deoxyspergualin (DSG), an immunosuppressive agent, has a peptidomimetic structure and binds specifically to Hsc70, which is thought to preclude the binding of certain other proteins to Hsc70 (Nadler et al., 1992). Immunoprecipitation assays were performed in the presence or absence of DSG to identify the interactions between Hsc70, p57, and cyclin D1 proteins in Myc-p57- or cyclin D1-overexpressing Lin^-CD34^- EML cells. Hsc70 bound to both p57 and cyclin D1, but DSG only inhibited the association between Hsc70 and cyclin D1 (Figure 6F). When freshly isolated BM $CD34^-$LSK cells were treated with DSG to inhibit the binding of Hsc70 to cyclin D1, cyclin D1 was imported into the nucleus and Rb became phosphorylated, whereas Hsc70 remained localized to the cytoplasm (Figure S6E). These data suggest that Hsc70 maintains the cytoplasmic localization of cyclin D1 through direct binding and functions as a specific G_0/G_1 factor relative to Rb phosphorylation in HSCs.

A nuclear localization signal (NLS) and a nuclear localization-related signal (NLRS) have been identified in amino acid regions 246–262 and 473–492, respectively, of Hsc70 (Tsukahara and Maru, 2004). Blocking of the NLRS, which functionally inhibits the nuclear export signal (NES), results in the inhibition of Hsc70 nuclear translocation (Figure S7A). GFP fusions were constructed of WT or NLRS-deficient (NLRS-D) Hsc70, which also binds to cyclin D1 (Figure S7B), and their subcellular localizations were examined in COS7 cells. WT Hsc70 localized to both the cytoplasm and the nucleus at 37°C and accumulated in the nucleus after heat shock at 42°C for 4 hr. In contrast, NLRS-D Hsc70 remained exclusively in the cytoplasm (Figure S7C).

Given that the nuclear translocation of Hsc70 was altered by the deletion of the NLRS, cell cycle progression was next compared in HSCs overexpressing WT or NLRS-D Hsc70. There was no significant difference in cell cycle status in culturing GFP^+LSK cells transduced with WT Hsc70 or NLRS-D Hsc70, compared to cells transduced with the GFP control vector (Figure S7D). We next examined the proliferation of the transduced cells 8 weeks after BMT. Analysis of the reconstituting BM showed an increase in the LSK fraction and a decrease in the $CD34^-$LSK cell population in mice transplanted with cells transduced with WT Hsc70. Ki67 staining showed that the percentage of G_0 cells in repopulating $CD34^-$LSK cells was significantly decreased by WT Hsc70, whereas deletion of the Hsc70 NLRS prevented the reduction in the number of $Ki67^-$ cells (Figure 7A). Furthermore, analysis of the donor-derived GFP^+ $CD34^-$LSK fraction showed that a significant increase in the percentage of $BrdU^+$ cells occurred in WT Hsc70-transduced cells but not in NLRS-D Hsc70- or control vector-transduced cells (Figure 7B). In addition, donor-derived $CD34^-$LSK formed few colonies in WT Hsc70- but not in NLRS-D Hsc70-transduced cohorts (Figure 7C). These data demonstrate that the subcellular localization of Hsc70 is critical for the maintenance of HSC cell cycle kinetics and repopulating capacity after BMT.

To examine the role of CDKs in these processes, the effect of the pharmacologic inhibition of CDK4/6 (with PD-0332991) or CDK2 (with BMS-387032) was evaluated in mice transplanted with HSCs overexpressing WT or NLRS-D Hsc70. Treatment in vivo with PD-0332991 significantly induced G_0 quiescence in HSCs expressing WT Hsc70, whereas BMS-387032 treatment increased the frequency of the G_1 population. In contrast, neither PD-0332991 nor BMS-387032 significantly affected the frequency of G_0 or G_1 cells in NLRS-D Hsc70-overexpressing HSCs, though the $S/G_2/M$ population was slightly suppressed by BMS-387032 in these cells (Figure 7D). In addition, $CD34^-$LSK cells were isolated from WT or DKO donor-derived

(B) Defective LSK repopulating activity of DKO cells. BMT experiments were performed as in (A). Data shown are the mean percentages (±SD) of donor-derived LSK cells at 16 weeks post-BMT (*$p < 0.01$, $n = 7$).
(C) Flow cytometric analysis of donor-derived BM fractions. The frequency of $CD48^-CD150^+$LSK cells was significantly reduced in reconstituting DKO BM as compared to other controls. Inserts shown are the mean percentages (±SD) of donor-derived LSK cells (*$p < 0.01$, $n = 7$).
(D) Proliferation status in donor-derived HSC and HPC populations. The cell cycle status of HSCs ($CD48^-CD150^+$LSK cells) or HPCs ($CD48^+$LSK cells) was determined by intracellular Hoechst staining. The mean percentage ± SD of cells in $S/G_2/M$ is indicated (*$p < 0.01$, $n = 7$).
(E) The percentage (±SD) of $CD4/CD8^+$ T cells, $B220^+$ B cells, or $Mac\text{-}1^+/Gr\text{-}1^+$ myeloid cells of donor-derived BM cells in BMT recipients (*$p < 0.01$, $n = 7$).
(F) Defective repopulating capacity of DKO LSK cells during serial BMT. The percentages (±SD) of donor-derived LSK cells were determined at 16 weeks after the second and third BMT (*$p < 0.01$, **$p < 0.05$, $n = 4$).

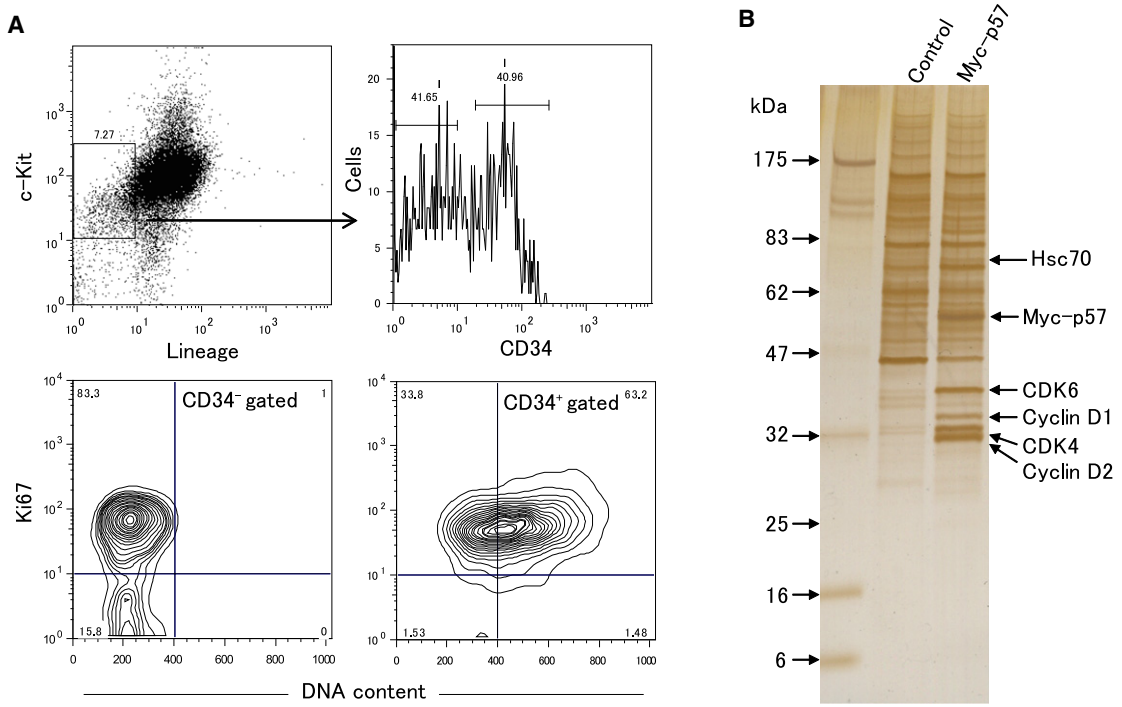
A
c-Kit
Lineage
7.27
Cells
CD34
41.65
40.96
Ki67
DNA content
CD34⁻ gated
CD34⁺ gated
83.3
15.8
33.8
1.53
1.48
63.2
B
Control
Myc-p57
kDa
175
83
62
47
32
25
16
6
Hsc70
Myc-p57
CDK6
Cyclin D1
CDK4
Cyclin D2
C
IP
IP
Lysate
Con-IgG
α-p57
Con-IgG
α-Hsc70
Hsc70
p57
D
HA-p57
HA-p27
HA-p21
IP
lysate
IgG
α-GFP
CDKIs
WB: α-HA
Hsc70
WB: α-GFP
E
% of pRb(+) cells in CD34⁻LSK
WT
p27⁻/⁻
p57⁻/⁻
DKO
pRb
Hsc70
Cyclin D1
Merge
WT
DKO
F
Control
Myc-p57
Myc-cyclin D1
DSG:
Hsc70
kDa
62
47
32
Myc-p57
Myc-cyclin D1
Hsc70 (Input)

BM at 4 months post-BMT. After 12 hr of culture with low-dose SCF (10 ng/ml) and with or without DSG, PD-0333991, and BMS-387032, cell cycle initiation was determined by Ki67 staining (Figure S7E). Treatment with PD-0332991 blocked the cell cycle progression induced by p27 and p57 deletion, whereas BMS-387032 had no effect on DKO cells. These data demonstrate that the CDK4/6 activity elicited by the nuclear expression of Hsc70/cyclin D1 releases HSCs from p27/p57-protecting quiescence. This model is additionally supported by the requirement for CDK4/6 but not CDK2 for cell cycle entry after DSG stimulation (Figure S7E).

DISCUSSION

Here, we report that the CDK inhibitors p57 and p27 cooperate to maintain HSC quiescence and that their function is closely correlated to the regulation of the cellular localization of the Hsc70/cyclin D1 complex in HSCs (Figure 7E).

Loss of p57 in FL HSCs Leads to Impaired Self-Renewal in Serial BMT, although the HSC Cell Cycle Is Not Affected

Upon mitogenic stimuli, D-type cyclins phosphorylate Rb, initiating G_0/G_1-S phase progression. Interestingly, HSCs abundantly express cytoplasmic cyclin D1, which is essential for HSC proliferation (Kozar et al., 2004) and which is correlated with the high expression of p57 in the cytoplasm of quiescent HSCs. In addition, SCF downregulates p57 and induces the nuclear translocation of cyclin D1 in HSCs (Figure S1). These findings suggest that, in quiescent HSCs, p57 and cyclin D1 form a complex in the cytoplasm and cyclin D1 is available for rapid re-entry into the cell cycle in response to mitogenic signals. Recent studies have indicated that the cytoplasmic localization of cyclin D1 plays an important role in cell cycle control (Tamamori-Adachi et al., 2003; Yamamoto et al., 2006). In addition, evidence for the cytoplasmic localization of p57 has been provided in normal and cancerous tissues (Pateras et al., 2009). Although a similar expression pattern has been reported for HSCs (Yamazaki et al., 2006), the exact functions of p57 are still not known.

The function of p57 was first examined with FL HSCs because *p57*-null mice show neonatal lethality. Unexpectedly, there were no significant abnormalities in the function of $p57^{-/-}$ HSCs, although a defect in repopulating capacity was observed in serial BMT. Moreover, no defects were detected in the cell cycle control of $p57^{-/-}$ donor-derived LSK cells, indicating the presence of alternative mechanisms to maintain quiescence (Figure 2). Interestingly, in the $p57^{-/-}$ donor-derived LSK cells, the levels of p27 and p18 were increased significantly, indicating that these proteins may functionally compensate for p57 in the maintenance of HSC quiescence. However, after administration of THPO to transplant recipient mice, the p18 level remained unchanged, whereas p27 expression was elevated in $p57^{-/-}$ LSK cells. Furthermore, the expression of p27 but not p18 in the cytoplasm of $p57^{-/-}$ HSCs was similar to that of p57 in WT HSCs, suggesting compensation for the lack of p57 by p27 (Figure 3). Indeed, p18 has been reported to play a negative role in self-renewal through an independent mechanism of cell cycle arrest in HSCs (Yuan et al., 2004). These finding suggest that p57 deficiency induces the exhaustion of HSCs after repeated BMTs by upregulating p18, and not defective HSC quiescence by p27 compensation. It remains to be determined why p57 deletion increases p18 during serial BMT and, more importantly, how p27 is functionally upregulated by p57 deletion to maintain HSC quiescence.

p57 and p27 Cooperate to Maintain Cell Cycle Quiescence and the Reconstitution Activity of HSCs

Both p27 and p57 have broad antiproliferative effects on a variety of cell types and tissues outside the hematopoietic system. Previous studies with mice lacking p27 and p57 have shown that these proteins cooperate to control the cell cycle in many tissues (Bilodeau et al., 2009; Zhang et al., 1998). In addition, it was demonstrated that p57 and p27 have overlapping functions in a knockin mouse model (Susaki et al., 2009). However, the physiological significance and the molecular mechanism for the cooperation between p27 and p57 in stem cells were not evaluated in previous studies.

In this study, the deficiency of both p57 and p27 resulted in a complete lack of long-term maintenance of HSCs, suggesting that these proteins cooperate to maintain HSC quiescence and protect HSCs from a loss of self-renewal activity (Figures 4 and 5). We have previously reported that Foxo3a, an important downstream target of PI3K-Akt signaling, is essential for the

Figure 6. Association of Hsc70 with p57, p27, and Cyclin D1

(A) Cell cycle analysis of $CD34^-$ and $CD34^+Lin^-$EML cells. Cells were stained with c-kit, CD34, and lineage (CD4, CD8, B220, TER-119, Gr-1, Mac-1) antibodies and analyzed by anti-Ki67 staining. Bottom panels indicate the cell cycle pattern of $CD34^-$ and $CD34^+Lin^-$EML cells.

(B) Detection of p57-associated proteins by mass spectrometry. The left lane contains molecular weight markers (sizes shown in kilodaltons), the middle lane contains proteins that nonspecifically bind to anti-myc beads in control EML lysates, and the right lane contains p57 complexes isolated from lysates from Myc-p57-infected EML cells. The positions of cyclin D1, cyclin D2, CDK4, CDK6, Myc-p57, and Hsc70 are indicated, along with the peptides identified by mass spectrometry.

(C) Hsc70 was detected in the p57 endogenous complex. Lin^-CD34^- EML cell lysates were immunoprecipitated with p57- or Hsc70-specific antibodies, and the bound complexes were immunoblotted for p57 or Hsc70.

(D) Hsc70 directly binds to p57 and p27. Expression vectors encoding EGFP-tagged Hsc70 and HA-tagged p21, p27, or p57 were cotransfected into COS-7 cells. EGFP-Hsc70 was immunoprecipitated with anti-GFP, and immunoblotting was carried out with HA or GFP antibodies.

(E) The phosphorylation of Rb is increased in $p27^{-/-}p57^{-/-}$ HSCs. $p27^{-/-}p57^{-/-}$ donor-derived $CD34^-$LSK cells were isolated by FACS at 16 weeks post-transplantation and stained with anti-Hsc70 (green), anti-cyclin D1 (red), anti-pRb (white), and DAPI (blue). Data shown are the mean (±SD) values from two independent experiments (*$p < 0.01$).

(F) DSG inhibits the association between Hsc70 and cyclin D1. EML cells were infected with Myc-p57 or Myc-cyclin D1 retroviruses and were cultured in the presence or absence of 10 μg/ml DSG for 24 hr. Immunoprecipitation with Myc antibodies was performed on the infected Lin^-CD34^- EML cells, and immunoblotting was carried out with Hsc70 or Myc antibodies.

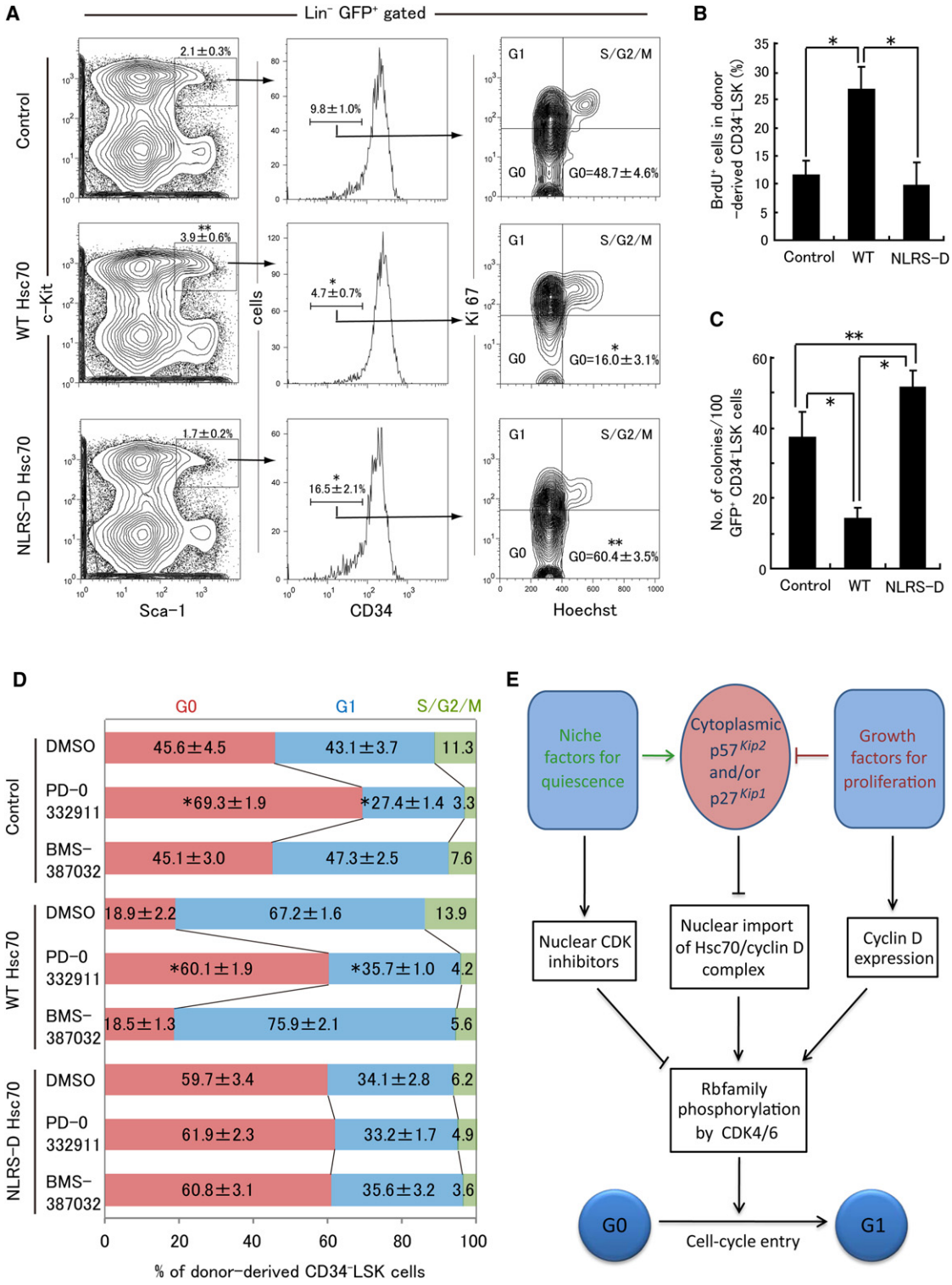

Figure 7. Control of Cytoplasmic Hsc70/Cyclin D1 Localization Is a Key Molecular Mechanism of HSC Quiescence

(A) Cell cycle analysis of donor-derived WT Hsc70 and NLRS-D Hsc70-transduced CD34$^-$LSK cells at 2 months after BMT. Inserts shown are the mean percentages (±SD) of donor-derived CD34$^-$LSK cells (*$p < 0.01$, **$p < 0.05$, $n = 4$).

(B) Increased frequency of BrdU$^+$ cells in the donor-derived WT-Hsc70 and NLRS-D Hsc70-transduced CD34$^-$LSK cells at 2 months after BMT. Recipient mice were intraperitoneally injected with 1 mg of BrdU at 2 months post-BMT. Twenty-four hours after injection, BM MNCs were harvested and stained with surface marker and BrdU antibodies and then analyzed by flow cytometry. The percentages (±SD) of BrdU$^+$ cells in donor-derived CD34$^-$LSK cells are indicated (*$p < 0.01$, $n = 4$).

maintenance of self-renewal capacity in HSCs. Maintenance of quiescence is defective in *Foxo3a*$^{-/-}$ HSCs, concomitant with the decreased expression of both p57 and p27 (Miyamoto et al., 2007). Another genetic model that illustrates the relationship between the PI3K-Akt pathway and HSC quiescence is the conditional knockout of PTEN, which regulates HSC maintenance by restricting HSC proliferation (Yilmaz et al., 2006; Zhang et al., 2006). The deficiency leads to the activation of PI3K, which results in Akt activation and consequently Foxo inactivation. This relationship may explain the similarities in the phenotypes of *PTEN*$^{-/-}$, *Foxo3a*$^{-/-}$, and *p27*$^{-/-}$*p57*$^{-/-}$ HSCs with respect to cell cycle regulation and repopulating capacity. More interestingly, the PI3K pathway also plays an important role in controlling the localization of cytoplasmic cyclin D1 in various cell lines (Radu et al., 2003; Yamamoto et al., 2006). These findings are especially interesting to us as the PI3K-Akt pathway acts upstream of p57 and p27 to control cyclin D1 localization in HSCs. The fact that both p57 and p27 function downstream of the same regulatory pathway may well be important. One possible explanation is that this compensatory mechanism exists to ensure that the cell cycle regulatory function of the PI3K pathway is intact even if one effector becomes inactivated.

Increased proliferation is often associated with the loss of self-renewal in HSCs, and alterations in the downstream regulators (Rb family members) of the CDK inhibitors are also associated with this phenotype (Viatour et al., 2008). Rb family proteins collectively regulate genes that normally inhibit the proliferation of both HSCs and hematopoietic progenitors. In contrast, p27 and p57 deficiency resulted in an altered cell cycle for HSCs but not for progenitors. These observations suggest that the cell cycle progression of HSCs and progenitors may be controlled by different mechanisms, although both processes are regulated by the Rb gene family.

Taken together, our results indicate that either p57 or its compensator p27 specifically plays a pivotal role in controlling HSC quiescence. This compensatory mechanism of p27 may provide an essential proliferation control in stem cells where p57 is not expressed at normal levels, as is the case in many human tumors and hyperplasia.

Importance of Hsc70, a p57 and p27 Binding Protein, in the Regulation of HSC Quiescence

Hsp70/Hsc70 chaperones localize to both cytosolic and nuclear compartments, where they regulate protein maturation, translocation, and association. Previous studies have shown that Hsp70 prevents the inactivation of the transcription factor GATA-1 by a caspase-mediated proteolysis, indicating that Hsp70 might indirectly trigger erythroid differentiation (Ribeil et al., 2007). Hsc70 also plays a role in the cytokine-mediated survival of hematopoietic progenitors by negatively influencing the stability of mRNA of the proapoptotic protein Bim, thus preventing apoptosis in hematopoiesis and leukemogenesis (Matsui et al., 2007). However, neither molecule has been shown to play a specific role in HSCs.

In this study, Hsc70 was identified as a p57 binding protein under quiescent conditions with the Lin$^-$CD34$^-$EML cells. Hsc70 is also associated with p27 and is involved in cell cycle progression (Figure 6D; Imamura et al., 2009). Moreover, Diehl et al. (2003) demonstrated that Hsc70-cyclin D1 binding can stabilize cyclin D1 and regulate its transport into the nucleus. Interestingly, Hsc70 and cyclin D1 formed a complex and additionally colocalized in the cytoplasm of quiescent HSCs. In future studies, identification of the stoichiometry of the p57/p27-Hsc70-cyclin D1 complex could help further investigations into the roles of these proteins in various contexts.

To determine whether the nuclear translocation of Hsc70 is functionally involved in the control of HSC quiescence, the cell cycle status of CD34$^-$LSK cells transduced with WT Hsc70 or NLRS-D Hsc70 were examined. The percentage of G_0 cells in WT Hsc70-transduced cells was significantly decreased and, interestingly, this effect was restored by the administration of a CDK4/6 inhibitor (PD-0332911) but not a CDK2 inhibitor (BMS-387032) (Figure 7). These results indicate that the subcellular localization of Hsc70, which regulates the activity of CDK4/6 by controlling the localization of cyclin D1, potentially acts downstream of p57 and p27 to control the quiescence of HSCs. Consistent with these observations, the enhanced proliferation of DKO HSCs compared to WT or single knockout HSCs is, at least in part, mediated by the nuclear import of the Hsc70/cyclin D1 complex (Figure 6E). Further, the treatment of HSCs with PD-0332991 blocked cell cycle progression induced by p27 and p57 deletion, whereas BMS-387032 had no effect on DKO cells. Collectively, our data suggest that p57 and p27 may regulate the activity of CDK4/6 by controlling the cellular localization of cyclin D1 through the association with Hsc70, resulting in the maintenance of HSC quiescence.

DSG, an Hsc70-binding immunosuppressive agent, inhibited the association between Hsc70 and cyclin D1 and resulted in the nuclear accumulation of cyclin D1 in HSCs, accompanied by Rb phosphorylation (Figure S6E). This finding further suggests that the appropriate distribution of cyclin D1 between the nucleus and cytoplasm is regulated by Hsc70 and is closely associated with cell cycle progression in HSCs. In addition, treatment with DSG in mice showed a potent BM suppression accompanying cyclin D1 degradation (data not shown), suggesting that the immunosuppressive properties of DSG are due, at least in part, to the disruption of the Hsc70-cyclin D1 interaction in BM cells.

Hsc70 has been considered to be a potential target in stem cell-based therapy. Expression of Hsc70, which is important

(C) Defective clonogenic capacity of donor-derived WT Hsc70-transduced CD34$^-$LSK cells HSCs in vitro. Donor-derived GFP control-, WT Hsc70-, or NLRS-D Hsc70-transduced CD34$^-$LSK cells were sorted at 2 months post-BMT and cultured in methylcellulose medium for 7 days. Data shown are the mean number of colonies (±SD) formed per 100 cells (*$p < 0.01$, **$p < 0.05$, $n = 3$).

(D) Cell cycle analysis of donor-derived GFP control-, WT Hsc70-, or NLRS-D Hsc70-transduced CD34$^-$LSK cells after administration of pharmacologic CDK inhibitors in vivo. Recipient mice were intraperitoneally injected with 100 mg/kg of PD-0332911 or BMS-387032 at 2 months post-BMT. Twenty-four hours after injection, BM MNCs were harvested and cell cycle progression was analyzed as in (A). The percentages (±SD) of G_0, G_1, and S/G_2/M phase cells in donor-derived CD34$^-$LSK cells are indicated (*$p < 0.01$, $n = 3$).

(E) Molecular regulation of the quiescence machinery in HSCs.

for the regulation of cyclin D1, is significantly upregulated in imatinib-resistant chronic myeloid leukemia (CML) cells (Pocaly et al., 2008). Furthermore, treatment with the Hsc70-specific inhibitor DSG in combination with imatinib decreases the viability of CML cells (José-Enériz et al., 2008). The slow cell cycle of leukemia stem cells may explain their resistance to anticancer drugs. Thus, the present study suggests that the manipulation of the cellular localization of Hsc70 and its binding to CDK inhibitors (p57 and p27) could serve as the basis for the development of new anticancer therapies.

EXPERIMENTAL PROCEDURES

Mice

Heterozygous $p57^{+/-}$ or $p27^{+/-}$ mice were crossed to generate $p57^{-/-}$ or $p27^{-/-}$ mice on a C57BL/6 background. C57BL/6 Ly5.1 congenic mice were purchased from Sankyo Lab Service (Tsukuba, Japan). Animal care was conducted in accordance with the guidelines of Keio University.

Flow Cytometry

Monoclonal antibodies (mAbs) recognizing the following markers were used for flow cytometric analyses and cell sorting (FACS Vantage or FACS AriaII, BD Bioscience): c-Kit (2B8), Sca-1 (E13-161.7), IL-7Rα (SB/199), CD16/CD32 (2.4G2), Ki67 (B56), CD4 (RM4-5), CD8 (53-6.7), B220 (RA3-6B2), TER-119 (Ly-76), Gr-1 (RB6-8C5), CD34 (RAM34), CD41 (MWReg30), CD48 (HM48-1), CD150 (TC15-12F12.2), CD45.1 (A20), CD45.2 (104), and anti-Mac-1 (M1/70). All mAbs were purchased from BD Biosciences. A mixture of mAbs recognizing CD4, CD8, B220, TER-119, Mac-1, and Gr-1 was used to identify Lin^+ cells. For cell cycle analyses, FL or BM cells were collected and stained for LSK. Cells were then fixed with 4% paraformaldehyde in PBS and stained with Ki67 and Hoechst33342 (Molecular Probes).

Quantitative Real-Time RCR Analysis

qRT-PCR was performed on a 7500 Fast Real-Time PCR System with a TaqMan Fast Universal PCR master mixture (Applied Biosystems). Relative expression of the selected genes was normalized to that of β-actin (FAM4352933) for each sample. The following TaqMan Gene Expression Assay Mixes were used: cyclin D1 (Mm03053889_sl), cyclin D2 (Mm00438070_ml), cyclin D3 (Mm01612362_ml), cyclin E1 (Mm00432367_ml), cyclin E2 (Mm00438077_ml), c-*myc* (Mm00487803_ml), p18 (Mm00483243_ml), p21 (Mm00432448_ml), p27 (Mm00438167_gl), p57 (Mm01272135_gl), Hsc70 (Mm01731394_gH), and Hsp70-1a (Mm01159846_sl).

Immunocytochemistry

Immunocytochemistry was performed as previously described (Hosokawa et al., 2010). The following antibodies were used for immunocytochemistry: anti-p57, anti-p27 and anti-p18 (Santa Cruz); anti-Hsc70 and anti-Hsp70 (Stressgen); anti-cyclin D1 and anti-p21 (BD Pharmigen); and anti-pRb (Sigma). Nuclei were identified by staining with DAPI. For the inhibition experiments, HSCs were cultured with 10 μg/ml DSG (Nippon Kayaku), 100 nM PD-0332991, or 100 nM BMS-387032 (Axon Medchem) before immunocytochemistry. Subcellular localizations were obtained with confocal laser scanning microscopy (FV1000, Olympus).

Mass Spectrometry

The LC-MS/MS analysis was performed as described previously (Sadaie et al., 2008).

Retroviral Transduction

Myc-p57, Myc-cyclin D1, and Hsc70 were ligated into the pMY-IRES-GFP vector, provided by Dr. Kitamura (University of Tokyo). Cyclin D1 cDNA was kindly provided by Dr. Ikeda (Tokyo Medical and Dental University). HA-p21, HA-p27, and HA-p57 in pcDNA3.1(+) vectors were kindly provided by Dr. Toyoshima (University of Tsukuba). Sequences of p57 shRNAs were as follows: sh-p57-1, 5′-GCAGGACGAGAATCAAGAG-3′; sh-p57-2, 5′-GAGAACTGCGCAGGAGAAC-3′; and sh-p57-3, 5′-CGACTTCTTCGCCAAGCGC-3′. Each sequence was separated from the corresponding reverse complement of the same 19-nucleotide sequence by a 9-nucleotide noncomplementary spacer (TTCAAGAGA). A scrambled sequence (5′-GACACGCGACTTGTACCAC-3′) served as the negative control. Oligonucleotides were cloned into the BglII and HindIII sites of the pReGS retrovirus vector. To retrovirally transduce LSK cells, isolated $p27^{+/+}$ or $p27^{-/-}$ LSK cells were cultured for 2 days, transfected on RetroNectin (Takara Bio Inc.)-coated plates via Magnetofection (OZ Biosciences), according to the manufacturer's instructions, and then cultured for 2 additional days. Cultures were maintained in SF-O3 medium containing 1.0% BSA, 100 ng/ml SCF, and 100 ng/ml THPO.

Colony-Forming Assays

For LTC-IC, 3×10^3 GFP^+LSK cells were cocultured with OP9 stromal cells, as previously described (Miyamoto et al., 2007). After 2–6 weeks in culture, cells were harvested and used in hematopoietic colony-forming assays.

Competitive Reconstitution Assay

Lethally irradiated C57BL/6 Ly5.1 congenic mice were reconstituted with FL-LSK cells from WT, $p27^{-/-}$, $p57^{-/-}$, or DKO mice (Ly5.2), in competition with BM MNCs from C57BL/6 Ly5.1 mice. For the serial transplantation analysis, donor-derived BM-LSK cells (4×10^3) were obtained from recipient mice at 16 weeks posttransplantation and transplanted into a second set of lethally irradiated mice. Subsequent transplantations were performed in the same manner.

Statistical Analysis

Significant differences between groups were determined with a two-tailed Student's t test.

SUPPLEMENTAL INFORMATION

Supplemental Information includes seven figures and can be found with this article online at doi:10.1016/j.stem.2011.07.003.

ACKNOWLEDGMENTS

This work was supported by a Grant-in-Aid for Scientific Research on Innovative Areas "Cancer Stem Cells" from the Ministry of Education, Culture, Sports, Science, and Technology (MEXT) of Japan, the Global COE program "Education and Research Center for Stem Cell Medicine" of Keio University, and a Grant-in-Aid for Japan Society for the Promotion of Science Fellows.

Received: August 13, 2010
Revised: February 15, 2011
Accepted: July 7, 2011
Published: September 1, 2011

REFERENCES

Adolfsson, J., Borge, O.J., Bryder, D., Theilgaard-Mönch, K., Astrand-Grundström, I., Sitnicka, E., Sasaki, Y., and Jacobsen, S.E. (2001). Upregulation of Flt3 expression within the bone marrow Lin(-)Sca1(+)c-kit(+) stem cell compartment is accompanied by loss of self-renewal capacity. Immunity *15*, 659–669.

Arai, F., Hirao, A., Ohmura, M., Sato, H., Matsuoka, S., Takubo, K., Ito, K., Koh, G.Y., and Suda, T. (2004). Tie2/angiopoietin-1 signaling regulates hematopoietic stem cell quiescence in the bone marrow niche. Cell *118*, 149–161.

Baharvand, H., Fathi, A., van Hoof, D., and Salekdeh, G.H. (2007). Concise review: Trends in stem cell proteomics. Stem Cells *25*, 1888–1903.

Bilodeau, S., Roussel-Gervais, A., and Drouin, J. (2009). Distinct developmental roles of cell cycle inhibitors p57Kip2 and p27Kip1 distinguish pituitary progenitor cell cycle exit from cell cycle reentry of differentiated cells. Mol. Cell. Biol. *29*, 1895–1908.

Cheng, T., Rodrigues, N., Dombkowski, D., Stier, S., and Scadden, D.T. (2000a). Stem cell repopulation efficiency but not pool size is governed by p27(kip1). Nat. Med. *6*, 1235–1240.

Cheng, T., Rodrigues, N., Shen, H., Yang, Y., Dombkowski, D., Sykes, M., and Scadden, D.T. (2000b). Hematopoietic stem cell quiescence maintained by p21cip1/waf1. Science *287*, 1804–1808.

Diehl, J.A., Yang, W., Rimerman, R.A., Xiao, H., and Emili, A. (2003). Hsc70 regulates accumulation of cyclin D1 and cyclin D1-dependent protein kinase. Mol. Cell. Biol. *23*, 1764–1774.

Hosokawa, K., Arai, F., Yoshihara, H., Iwasaki, H., Hembree, M., Yin, T., Nakamura, Y., Gomei, Y., Takubo, K., Shiama, H., et al. (2010). Cadherin-based adhesion is a potential target for niche manipulation to protect hematopoietic stem cells in adult bone marrow. Cell Stem Cell *6*, 194–198.

Imamura, Y., Fujigaki, Y., Oomori, Y., Usui, S., and Wang, P.L. (2009). Cooperation of salivary protein histatin 3 with heat shock cognate protein 70 relative to the G1/S transition in human gingival fibroblasts. J. Biol. Chem. *284*, 14316–14325.

Iwasaki, H., Arai, F., Kubota, Y., Dahl, M., and Suda, T. (2010). Endothelial protein C receptor-expressing hematopoietic stem cells reside in the perisinusoidal niche in fetal liver. Blood *116*, 544–553.

José-Enériz, E.S., Román-Gómez, J., Cordeu, L., Ballestar, E., Gárate, L., Andreu, E.J., Isidro, I., Guruceaga, E., Jiménez-Velasco, A., Heiniger, A., et al. (2008). BCR-ABL1-induced expression of HSPA8 promotes cell survival in chronic myeloid leukaemia. Br. J. Haematol. *142*, 571–582.

Kiel, M.J., Yilmaz, O.H., Iwashita, T., Yilmaz, O.H., Terhorst, C., and Morrison, S.J. (2005). SLAM family receptors distinguish hematopoietic stem and progenitor cells and reveal endothelial niches for stem cells. Cell *121*, 1109–1121.

Kozar, K., Ciemerych, M.A., Rebel, V.I., Shigematsu, H., Zagozdzon, A., Sicinska, E., Geng, Y., Yu, Q., Bhattacharya, S., Bronson, R.T., et al. (2004). Mouse development and cell proliferation in the absence of D-cyclins. Cell *118*, 477–491.

Malumbres, M., Sotillo, R., Santamaría, D., Galán, J., Cerezo, A., Ortega, S., Dubus, P., and Barbacid, M. (2004). Mammalian cells cycle without the D-type cyclin-dependent kinases Cdk4 and Cdk6. Cell *118*, 493–504.

Matsui, H., Asou, H., and Inaba, T. (2007). Cytokines direct the regulation of Bim mRNA stability by heat-shock cognate protein 70. Mol. Cell *25*, 99–112.

Miyamoto, K., Araki, K.Y., Naka, K., Arai, F., Takubo, K., Yamazaki, S., Matsuoka, S., Miyamoto, T., Ito, K., Ohmura, M., et al. (2007). Foxo3a is essential for maintenance of the hematopoietic stem cell pool. Cell Stem Cell *1*, 101–112.

Nadler, S.G., Tepper, M.A., Schacter, B., and Mazzucco, C.E. (1992). Interaction of the immunosuppressant deoxyspergualin with a member of the Hsp70 family of heat shock proteins. Science *258*, 484–486.

Oguro, H., Iwama, A., Morita, Y., Kamijo, T., van Lohuizen, M., and Nakauchi, H. (2006). Differential impact of Ink4a and Arf on hematopoietic stem cells and their bone marrow microenvironment in Bmi1-deficient mice. J. Exp. Med. *203*, 2247–2253.

Passegué, E., Wagers, A.J., Giuriato, S., Anderson, W.C., and Weissman, I.L. (2005). Global analysis of proliferation and cell cycle gene expression in the regulation of hematopoietic stem and progenitor cell fates. J. Exp. Med. *202*, 1599–1611.

Pateras, I.S., Apostolopoulou, K., Niforou, K., Kotsinas, A., and Gorgoulis, V.G. (2009). p57KIP2: "Kip"ing the cell under control. Mol. Cancer Res. *7*, 1902–1919.

Pocaly, M., Lagarde, V., Etienne, G., Dupouy, M., Lapaillerie, D., Claverol, S., Vilain, S., Bonneu, M., Turcq, B., Mahon, F.X., and Pasquet, J.M. (2008). Proteomic analysis of an imatinib-resistant K562 cell line highlights opposing roles of heat shock cognate 70 and heat shock 70 proteins in resistance. Proteomics *8*, 2394–2406.

Radu, A., Neubauer, V., Akagi, T., Hanafusa, H., and Georgescu, M.M. (2003). PTEN induces cell cycle arrest by decreasing the level and nuclear localization of cyclin D1. Mol. Cell. Biol. *23*, 6139–6149.

Ribeil, J.A., Zermati, Y., Vandekerckhove, J., Cathelin, S., Kersual, J., Dussiot, M., Coulon, S., Moura, I.C., Zeuner, A., Kirkegaard-Sørensen, T., et al. (2007). Hsp70 regulates erythropoiesis by preventing caspase-3-mediated cleavage of GATA-1. Nature *445*, 102–105.

Sadaie, M., Shinmyozu, K., and Nakayama, J. (2008). A conserved SET domain methyltransferase, Set11, modifies ribosomal protein Rpl12 in fission yeast. J. Biol. Chem. *283*, 7185–7195.

Scandura, J.M., Boccuni, P., Massagué, J., and Nimer, S.D. (2004). Transforming growth factor beta-induced cell cycle arrest of human hematopoietic cells requires p57KIP2 up-regulation. Proc. Natl. Acad. Sci. USA *101*, 15231–15236.

Susaki, E., Nakayama, K., Yamasaki, L., and Nakayama, K.I. (2009). Common and specific roles of the related CDK inhibitors p27 and p57 revealed by a knock-in mouse model. Proc. Natl. Acad. Sci. USA *106*, 5192–5197.

Tamamori-Adachi, M., Ito, H., Sumrejkanchanakij, P., Adachi, S., Hiroe, M., Shimizu, M., Kawauchi, J., Sunamori, M., Marumo, F., Kitajima, S., and Ikeda, M.A. (2003). Critical role of cyclin D1 nuclear import in cardiomyocyte proliferation. Circ. Res. *92*, e12–e19.

Tsukahara, F., and Maru, Y. (2004). Identification of novel nuclear export and nuclear localization-related signals in human heat shock cognate protein 70. J. Biol. Chem. *279*, 8867–8872.

Viatour, P., Somervaille, T.C., Venkatasubrahmanyam, S., Kogan, S., McLaughlin, M.E., Weissman, I.L., Butte, A.J., Passegué, E., and Sage, J. (2008). Hematopoietic stem cell quiescence is maintained by compound contributions of the retinoblastoma gene family. Cell Stem Cell *3*, 416–428.

Yamamoto, M., Tamakawa, S., Yoshie, M., Yaginuma, Y., and Ogawa, K. (2006). Neoplastic hepatocyte growth associated with cyclin D1 redistribution from the cytoplasm to the nucleus in mouse hepatocarcinogenesis. Mol. Carcinog. *45*, 901–913.

Yamazaki, S., Iwama, A., Takayanagi, S., Morita, Y., Eto, K., Ema, H., and Nakauchi, H. (2006). Cytokine signals modulated via lipid rafts mimic niche signals and induce hibernation in hematopoietic stem cells. EMBO J. *25*, 3515–3523.

Yamazaki, S., Iwama, A., Takayanagi, S., Eto, K., Ema, H., and Nakauchi, H. (2009). TGF-beta as a candidate bone marrow niche signal to induce hematopoietic stem cell hibernation. Blood *113*, 1250–1256.

Ye, Z.J., Kluger, Y., Lian, Z., and Weissman, S.M. (2005). Two types of precursor cells in a multipotential hematopoietic cell line. Proc. Natl. Acad. Sci. USA *102*, 18461–18466.

Yilmaz, O.H., Valdez, R., Theisen, B.K., Guo, W., Ferguson, D.O., Wu, H., and Morrison, S.J. (2006). Pten dependence distinguishes haematopoietic stem cells from leukaemia-initiating cells. Nature *441*, 475–482.

Yoshihara, H., Arai, F., Hosokawa, K., Hagiwara, T., Takubo, K., Nakamura, Y., Gomei, Y., Iwasaki, H., Matsuoka, S., Miyamoto, K., et al. (2007). Thrombopoietin/MPL signaling regulates hematopoietic stem cell quiescence and interaction with the osteoblastic niche. Cell Stem Cell *1*, 685–697.

Yuan, Y., Shen, H., Franklin, D.S., Scadden, D.T., and Cheng, T. (2004). In vivo self-renewing divisions of haematopoietic stem cells are increased in the absence of the early G1-phase inhibitor, p18INK4C. Nat. Cell Biol. *6*, 436–442.

Zhang, P., Wong, C., DePinho, R.A., Harper, J.W., and Elledge, S.J. (1998). Cooperation between the Cdk inhibitors p27(KIP1) and p57(KIP2) in the control of tissue growth and development. Genes Dev. *12*, 3162–3167.

Zhang, J., Grindley, J.C., Yin, T., Jayasinghe, S., He, X.C., Ross, J.T., Haug, J.S., Rupp, D., Porter-Westpfahl, K.S., Wiedemann, L.M., et al. (2006). PTEN maintains haematopoietic stem cells and acts in lineage choice and leukaemia prevention. Nature *441*, 518–522.